Int. J. Solids Structures, 1968, Vol. 4, pp. 139 to 157. Pergamon Press. Printed in Great Britain

AN APPROXIMATE SOLUTION FOR THE EFFECT OF "SHEAR LAG" IN THE MEASUREMENT OF RESIDUAL STRESSES USING A PHOTOELASTIC GAUGE

C. J. HOOKE

Department of Mechanical Engineering, University of Birmingham, Birmingham

and

J. J. STAGG*

Welwyn Electric Ltd.

Abstract—An approximate method of allowing for the effect of shear lag in photoelastic gauges is described. Numerical results are presented for a wide range of gauge geometries.

NOTATION

a	hole radius
b	gauge outside radius
f	fringe-stress coefficient for gauge material
g_n, h_n, i_n	stress coefficients defined by equations (13) and (35)
n	load harmonic
r	radius
t	gauge thickness
u	radial displacement
v	circumferential displacement
w	axial displacement
z	axial co-ordinate
B	b/a
$A(r/a)$, $B(r/a)$, $C(r/a)$	fringe coefficients defined by equations (17) and (37)
N	fringe order
R	r/a
S_1, S_2	principal residual stresses
T	t/a
U	u/a
V	v/a
W	w/a
Z	z/a
ξ, ϕ	displacement functions
θ	angular co-ordinate
τ	stress (the notation used is that of Ref. [9])
μ, λ	Lamé elastic constants

Subscripts

g	gauge
b	metal
n	load harmonic

* Formerly at: Joseph Lucas Group Research Centre.

INTRODUCTION

A METHOD of measuring residual stresses in metals using photoelastic strain gauges has been developed by Nisida [1] Nisida and Takabayashi [2] and by Gibbs *et al.* [3]. In this method an annular disc of Araldite, or similar photoelastic material, is bonded onto the surface of the metal in which the residual stresses are to be measured. A hole is then drilled into the material underlying the central hole in the gauge. The removal of this metal produces strains round the hole which are transmitted to the photoelastic material.

If the gauge is now viewed in polarised light, using a conventional reflection polariscope, a fringe pattern is seen. This fringe pattern can be used to determine the magnitudes and directions of the principal residual stresses in the metal.

The technique has the advantage of being practically non-destructive and requires no special skills or equipment.

Unfortunately, although the strains present in the base material are transmitted faithfully to the lower surface of the gauge, there is a progressive diminution of strain through the thickness of the gauge. This effect, known as "shear lag," makes the interpretation of the fringe patterns using elementary plane strain theory impossible. It is the purpose of this paper to describe a method whereby the effects of shear lag can be estimated and to obtain a simple relation between the fringe order measured and the residual stresses present in the material.

THEORY

In order to make the problem more tractable the residual stresses are assumed uniform in the region of the gauge and are regarded as being a linear combination of two basic stress systems. The first system has both principal stresses equal to unity and the second system has the principal stresses equal to unity but of opposite sign. With the fringe patterns calculated for these two systems, the fringe pattern for any other stress system can be obtained by superposition. Conversely, the stresses producing a particular fringe pattern may be estimated by reducing the measured fringe pattern to an appropriate combination of the two basic patterns and taking the same combination of the stress systems.

Before starting the analysis of the gauge it is expedient to introduce the following non-dimensional parameters:

$$R = \frac{r}{a} \quad Z = \frac{z}{a} \quad U = \frac{u}{a} \quad V = \frac{v}{a} \quad W = \frac{w}{a} \quad T = \frac{t}{a} \quad B = \frac{b}{a}. \tag{1}$$

EQUAL PRINCIPAL STRESSES

When the hole is drilled the change of stress at the hole boundary is equal to the reverse of the original stress in the material. For most photoelastic materials the modulus of elasticity of the gauge will be small compared with that of the metal, and the reinforcing effect of the gauge on the underlying metal may be ignored. The displacements round the hole, for unit residual stress, will therefore be:

$$\begin{aligned} U &= \frac{1}{2\mu_b}\frac{1}{R} \\ W &= 0. \end{aligned} \tag{2}$$

These displacements will form the boundary conditions at the base of the gauge. At all the other gauge boundaries the loads will be zero, giving:

$$\begin{aligned}
&\text{at } Z = T && \tau_{RZ} = 0 \\
& && \tau_{ZZ} = 0 \\
&\text{at } R = 1 && \tau_{RR} = 0 \\
& && \tau_{RZ} = 0 \\
&\text{at } R = B && \tau_{RR} = 0 \\
& && \tau_{RZ} = 0.
\end{aligned} \tag{3}$$

The problem of axially varying loads on short cylinders, of which this is an example, has been extensively investigated by Filon [4], Galerkin [5], Prokopov [6], Barton [7] and Lur'e [8] and many other authors and it appears that exact solutions are possible only for some special loading conditions. The boundary conditions expressed in equations (2) and (3) do not form one of these loading conditions and an approximate solution must be sought.

Since the vertical deflection at the base of the gauge is zero, and the gauge is relatively thin, an obvious approximation is to equate the axial displacements to zero everywhere in the gauge. While this will produce considerable errors in the axial stress, the error in the difference between the radial and circumferential stresses should be relatively small, and hence the fringe order should be predicted with sufficient accuracy. With the assumption of zero axial displacement, axial body forces have to be introduced and the axial loads on the boundaries no longer influence the displacements of the gauge. The boundary conditions therefore reduce to:

$$\begin{aligned}
&\text{at } Z = 0 && U = \frac{1}{2\mu_b} \times \frac{1}{R} \\
&\text{at } Z = T && \tau_{RZ} = 0 \\
&\text{at } R = 1 && \tau_{RR} = 0 \\
&\text{at } R = B && \tau_{RR} = 0
\end{aligned} \tag{4}$$

These conditions can be satisfied by a cyclic load of:

$$\begin{aligned}
&\text{at } R = 1 && \tau_{RR} = -2\mu_g/\mu_b && (4n-2) < Z < 4nT \\
& && \tau_{RR} = 0 && 4nT < Z < (4n+2)T \\
&\text{at } R = B && \tau_{RR} = -2\mu_g/\mu_b \times \frac{1}{B^2} && (4n-2) < Z < 4nT \\
& && \tau_{RR} = 0 && 4nT < Z < (4n+2)T
\end{aligned} \tag{5}$$

where n is an integer, acting on an infinite cylinder of the same outside and inside diameters as the gauge. From considerations of symmetry the shear stress on the $Z = T$ face will be zero and the displacements at the $Z = 0$ face will be equal to those produced by the mean load. On expanding the above loading into two Fourier's series the expressions for radial

stress at the inner and outer surfaces of the cylinder become:

$$\begin{aligned} &\text{at } R = 1 && \tau_{RR} = -\mu_g/\mu_b\left[1-\frac{4}{\pi}\sum_{n=1,3,\ldots}^{\infty}\frac{1}{n}\sin\left(n\pi\frac{Z}{2T}\right)\right] \\ &\text{at } R = B && \tau_{RR} = -\mu_g/\mu_b\left[1-\frac{4}{\pi}\sum_{n=1,3,\ldots}^{\infty}\frac{1}{n}\sin\left(n\pi\frac{Z}{2T}\right)\right]\frac{1}{B^2}. \end{aligned} \tag{6}$$

For the non-cyclic terms of these series the difference between the radial and circumferential stress is:

$$\tau_{RR}-\tau_{\theta\theta} = -2\mu_g/\mu_b\frac{1}{R^2}. \tag{7}$$

To find the equivalent stress difference for the cyclic terms, consider a loading of the form:

$$\begin{aligned} &\text{at } R = 1 && \tau_{RR} = \sin(kZ) \\ &\text{at } R = B && \tau_{RR} = \frac{1}{B^2}\sin(kZ). \end{aligned} \tag{8}$$

This loading, which by appropriate choice of k can be made to represent any of the terms of the series, will produce a radial displacement in the cylinder;

$$U = \frac{1}{\mu_g}\phi\sin(kZ) \tag{9}$$

where ϕ is a function of R only.

Assuming that the gauge material is homogeneous and isotropic, the radial, circumferential, and shear stresses are obtained from equation (9) together with the condition that the axial displacement is zero:

$$\begin{aligned} \tau_{RR} &= \left[(2+\lambda_g/\mu_g)\frac{d\phi}{dR}+\frac{\lambda_g}{\mu_g}\frac{\phi}{R}\right]\sin(kZ) \\ \tau_{\theta\theta} &= \left[(2+\lambda_g/\mu_g)\frac{\phi}{R}+\frac{\lambda_g}{\mu_g}\frac{d\phi}{dR}\right]\sin(kZ) \\ \tau_{RZ} &= k\phi\cos(kZ). \end{aligned} \tag{10}$$

On substituting these stresses into the equation for radial equilibrium a differential equation for ϕ is obtained:

$$\frac{d^2\phi}{dR^2}+\frac{1}{R}\frac{d\phi}{dR}-\frac{1}{R^2}\phi-k^2\phi\left(2+\frac{\lambda_g}{\mu_g}\right) = 0. \tag{11}$$

The boundary conditions that must be satisfied by ϕ at $R = 1$ and $R = B$ can be obtained

from equations (8). These equations yield:

$$\text{at } R = 1 \qquad \left(2+\frac{\lambda_g}{\mu_g}\right)\frac{d\phi}{dR}+\frac{\lambda_g}{\mu_g}\phi = 1$$

$$\text{at } R = B \qquad \left(2+\frac{\lambda_g}{\mu_g}\right)\frac{d\phi}{dR}+\frac{\lambda_g}{\mu_g}\frac{\phi}{B} = \frac{1}{B^2} \tag{12}$$

Equation (11) was solved numerically for these boundary conditions using the Gill–Kutta procedure, and the values of ϕ/R and $d\phi/dR$ obtained for a number of values of radius.

At a given radius the difference between the radial and circumferential stresses for the load given by equations (8) will be:

$$\tau_{RR}-\tau_{\theta\theta} = 2\left(\frac{d\phi}{dR}-\frac{\phi}{R}\right)\sin(kZ) \tag{13}$$

Denoting $2(d\phi/dR-\phi/R)$ by $g_n(R)$ for the case where k is equal to $n\pi/2T$ the principal stress difference due to the total load on the cylinder becomes:

$$\tau_{RR}-\tau_{\theta\theta} = -\frac{\mu_g}{\mu_b}\left[\frac{2}{R^2}-\frac{4}{\pi}\sum_{n=1,3,5\ldots}^{\infty}\frac{1}{n}g_n(R)\sin\left(n\pi\frac{Z}{2T}\right)\right] \tag{14}$$

This equation represents the principal stress difference at every point in the gauge. However the photoelastic effect observed depends on the product of the thickness of the gauge and the mean value of the principal stress difference. This mean principal stress difference is given by:

$$(\tau_{RR}-\tau_{\theta\theta})_{\text{mean}} = \frac{1}{T}\int_0^T(\tau_{RR}-\tau_{\theta\theta})\,dZ \tag{15}$$

which on integration becomes:

$$(\tau_{RR}-\tau_{\theta\theta})_{\text{mean}} = -\frac{\mu_g}{\mu_b}\left[\frac{2}{R^2}-\frac{8}{\pi^2}\sum_{n=1,3,5\ldots}^{\infty}\frac{1}{n^2}g_n(R)\right] \tag{16}$$

In calculating the stress difference, the series was truncated after sufficient terms had been summed for the error to be below 1%. For most gauges less than ten terms were required.

Writing $A(r/a)$ for the sum

$$\left[-\frac{2}{R^2}+\frac{8}{\pi^2}\sum\frac{1}{n^2}g_n(R)\right]$$

the actual fringe order (N) for a photoelastic material of fringe stress coefficient f and thickness t will be:

$$N = \frac{2t}{f}\frac{\mu_g}{\mu_b}\qquad A(r/a). \tag{17}$$

The value of $A(r/a)$ is plotted against r/a for a range of values of t/a for an araldite gauge of large outside radius in Fig. 1. In Fig. 2 the value of $(t/a)A(r/a)$, which for a constant hole diameter is proportional to the actual fringe order, is plotted against t/a.

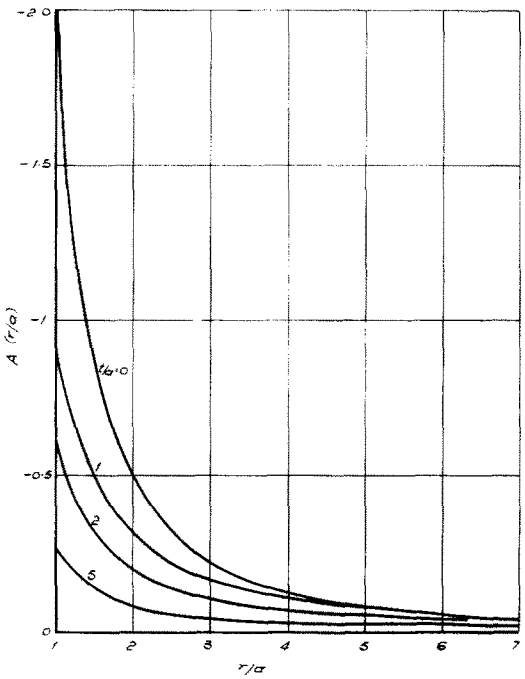

FIG. 1. Variation of $A(r/a)$ with radius.

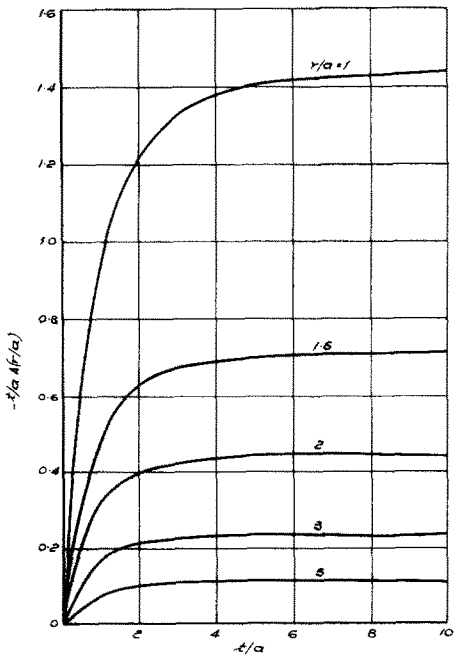

FIG. 2. Effect of gauge thickness on t/a $A(r/a)$.

EQUAL BUT OPPOSITE PRINCIPAL RESIDUAL STRESSES OF UNIT MAGNITUDE

The analysis in this case is identical in principal to that employed in the previous section. However, an additional complication is introduced since angular displacements of the gauge and metal must be considered.

The first step is to calculate the displacements of the metal at the metal–gauge interface due to drilling the hole. Prior to the removal of the metal the stresses at the hole boundary are:

$$\begin{aligned} \tau_R &= \cos 2\theta \\ \tau_{R\theta} &= -\sin 2\theta. \end{aligned} \tag{18}$$

When the hole is drilled these stresses are removed and strains produced round the hole. Unless Poisson's ratio for the metal is zero there is no simple exact method of calculating the displacements at the metal surface. However, following the technique of the previous section it is assumed that the axial displacements are zero and with this assumption the displacements of the metal will be:

$$\begin{aligned} U &= \frac{1}{2\mu_b}\left(\frac{(\lambda_b+2\mu_b)}{(\lambda_b+\mu_b)}\frac{2}{R}-\frac{1}{R^3}\right)\cos 2\theta \\ V &= \frac{1}{2\mu_b}\left(-\frac{2\mu_b}{\lambda_b+\mu_b}\frac{1}{R}-\frac{1}{R^3}\right)\sin 2\theta \\ W &= 0. \end{aligned} \tag{19}$$

These displacements form the boundary conditions at the base of the gauge. At the other boundaries the loads will be zero giving:

$$\begin{aligned} &\text{at } R = 1 && \tau_{RR} = \tau_{RZ} = \tau_{R\theta} = 0 \\ &\text{at } R = B && \tau_{RR} = \tau_{RZ} = \tau_{R\theta} = 0 \\ &\text{at } Z = T && \tau_{RZ} = \tau_{ZZ} = \tau_{Z\theta} = 0. \end{aligned} \tag{20}$$

As in the previous section the axial displacements are assumed zero throughout the gauge and the boundary conditions reduced to:

$$\begin{aligned} &\text{at } R = 1 && \tau_{RR} = \tau_{R\theta} = 0 \\ &\text{at } R = B && \tau_{RR} = \tau_{R\theta} = 0 \\ &\text{at } Z = 0 && U = \frac{1}{2\mu_b}\left[\frac{(\lambda_b+2\mu_b)}{(\lambda_b+\mu_b)}\frac{2}{R}-\frac{1}{R^3}\right]\cos 2\theta \\ & && V = \frac{1}{2\mu_b}\left[-\frac{2\mu_b}{\lambda_b+\mu_b}\frac{1}{R}-\frac{1}{R^3}\right]\sin 2\theta \\ &\text{at } Z = T && \tau_{RZ} = \tau_{Z\theta} = 0. \end{aligned} \tag{21}$$

The next step is to obtain a loading on an infinite cylinder, of the same inside and outside diameters as the gauge, that will satisfy these boundary conditions. Considering an infinitely long cylinder of gauge material with uniform displacements equal to those

at the metal–gauge interface, the stresses are found to be:

$$\begin{aligned}
\tau_{RR} &= \left[\frac{\mu_g}{\mu_b}\frac{3}{R^4} - \left(\frac{\mu_g}{\mu_b} + \frac{\lambda_g+\mu_g}{\lambda_b+\mu_b}\right)\frac{2}{R^2}\right]\cos 2\theta \\
\tau_{\theta\theta} &= \left[-\frac{\mu_g}{\mu_b}\frac{3}{R^4} + \left(\frac{\mu_g}{\mu_b} - \frac{\lambda_g+\mu_g}{\lambda_b+\mu_b}\right)\frac{2}{R^2}\right]\cos 2\theta \\
\tau_{R\theta} &= \left[\frac{\mu_g}{\mu_b}\frac{3}{R^4} - \frac{\mu_g}{\mu_b}\frac{2}{R^2}\right]\sin 2\theta.
\end{aligned} \tag{22}$$

On substituting these stresses into the equations for radial and circumferential equilibrium, the body forces in the cylinder are obtained:

$$\begin{aligned}
F_R &= 2D\frac{\mu_g}{\mu_b}\frac{1}{R^3}\cos 2\theta \\
F_\theta &= 2D\frac{\mu_g}{\mu_b}\frac{1}{R^3}\sin 2\theta
\end{aligned} \tag{23}$$

where

$$D = 2\left[\frac{\mu_g}{\mu_b} - \frac{\lambda_g+\mu_g}{\lambda_b+\mu_b}\right]\frac{\mu_b}{\mu_g}.$$

The boundary conditions expressed in equations (21), and the absence of body forces from $Z = 0$ to $Z = T$, can therefore be satisfied by loading the boundaries of an infinitely long cylinder as follows:

$$\begin{array}{lll}
\text{at } R = 1 & \tau_{RR} = 0 & 4nT < Z < (4n+2)T \\
& \tau_{RR} = 2(D-1)\dfrac{\mu_g}{\mu_b}\cos 2\theta & (4n-2)T < Z < 4nT \\
& \tau_{R\theta} = 0 & 4nT < Z < (4n+2)T \\
& \tau_{R\theta} = 2\dfrac{\mu_g}{\mu_b}\sin 2\theta & (4n-2)T < Z < 4nT \\
\text{at } R = B & \tau_{RR} = 0 & 4nT < Z < (4n+2)T \\
& \tau_{RR} = 2\left[(D-4)\dfrac{1}{B^2} + 3\dfrac{1}{B^4}\right]\dfrac{\mu_g}{\mu_b}\cos 2\theta & (4n-2)T < Z < 4nT \\
& \tau_{R\theta} = 0 & 4nT < Z < (4n+2)T \\
& \tau_{R\theta} = 2\left[-\dfrac{2}{B^2} + \dfrac{3}{B^4}\right]\dfrac{\mu_g}{\mu_b}\sin 2\theta & (4n-2)T < Z < 4nT
\end{array} \tag{24}$$

where n is an integer, and by applying the following body forces inside the cylinder:

$$\left.\begin{aligned} F_R &= F_\theta = 0 && 4nT < Z < (4n+2)T \\ F_R &= 4D\frac{\mu_g}{\mu_b}\frac{1}{R^3}\cos 2\theta \\ F_\theta &= 4D\frac{\mu_g}{\mu_b}\frac{1}{R^3}\sin 2\theta \end{aligned}\right\} \quad (4n-2)T < Z < 4nT. \tag{25}$$

Expanding these loads and forces into Fourier's series yields:

$$\begin{aligned} \text{at } R = 1 \qquad \tau_{RR} &= (D-1)\frac{\mu_g}{\mu_b}\left[1-\frac{4}{\pi}\sum_{n=1,3,5}^{\infty}\frac{1}{n}\sin\left(n\pi\frac{Z}{2T}\right)\right]\cos 2\theta \\ \tau_{R\theta} &= \frac{\mu_g}{\mu_b}\left[1-\frac{4}{\pi}\sum_{n=1,3,5}^{\infty}\frac{1}{n}\sin\left(n\pi\frac{Z}{2T}\right)\right]\sin 2\theta \\ \text{at } R = B \qquad \tau_{RR} &= \left[(D-4)\frac{1}{B^2}+\frac{3}{B^4}\right]\frac{\mu_g}{\mu_b}\left[1-\frac{4}{\pi}\sum_{n=1,3,5}^{\infty}\frac{1}{n}\sin\left(n\pi\frac{Z}{2T}\right)\right]\cos 2\theta \\ \tau_{R\theta} &= \left[-\frac{2}{B^2}+\frac{3}{B^4}\right]\frac{\mu_g}{\mu_b}\left[1-\frac{4}{\pi}\sum_{n=1,3,5}^{\infty}\frac{1}{n}\sin\left(n\pi\frac{Z}{2T}\right)\right]\sin 2\theta \end{aligned} \tag{26}$$

and in the body of the cylinder

$$\begin{aligned} F_R &= 2D\frac{\mu_g}{\mu_b}\frac{1}{R^3}\left[1-\frac{4}{\pi}\sum_{n=1,3,5}^{\infty}\frac{1}{n}\sin\left(n\pi\frac{Z}{2T}\right)\right]\cos 2\theta \\ F_\theta &= 2D\frac{\mu_g}{\mu_b}\frac{1}{R^3}\left[1-\frac{4}{\pi}\sum_{n=1,3,5}^{\infty}\frac{1}{n}\sin\left(n\pi\frac{Z}{2T}\right)\right]\sin 2\theta. \end{aligned} \tag{27}$$

For the non-cyclic terms the stresses are given by equation (22), and the difference between the radial, and circumferential stresses, and the shear stress are:

$$\begin{aligned} (\tau_{RR}-\tau_{\theta\theta}) &= \frac{\mu_g}{\mu_b}\left[-\frac{4}{R^2}+\frac{6}{R^4}\right]\cos 2\theta \\ \tau_{R\theta} &= \frac{\mu_g}{\mu_b}\left[-\frac{2}{R^2}+\frac{3}{R^4}\right]\sin 2\theta. \end{aligned} \tag{28}$$

To find the equivalent values for the cyclic terms consider a loading:

$$\begin{aligned} \text{at } R = 1 \qquad \tau_{RR} &= (D-1)\sin kZ\cos 2\theta \\ \tau_{R\theta} &= \sin kZ\sin 2\theta \\ \text{at } R = B \qquad \tau_{RR} &= \left[(D-4)\frac{1}{B^2}+\frac{3}{B^4}\right]\sin kZ\cos 2\theta \\ \tau_{R\theta} &= \left[-\frac{2}{B^2}+\frac{3}{B^4}\right]\sin kZ\sin 2\theta \end{aligned} \tag{29}$$

and body forces

$$F_R = \frac{2D}{R^3} \sin kZ \cos 2\theta$$
$$F_\theta = \frac{2D}{R^3} \sin kZ \sin 2\theta. \tag{30}$$

This loading, which by appropriate choice of k can be made to represent any of the cyclic loads, will produce displacements:

$$U = \frac{1}{\mu_g} \phi \sin kZ \cos 2\theta$$
$$V = \frac{1}{\mu_g} \xi \sin kZ \sin 2\theta \tag{31}$$

where ϕ and ξ are functions of R only. Assuming that the gauge material is homogeneous and isotropic the stresses may be obtained from these displacements, together with the condition of zero axial strain:

$$\tau_{RR} = \left[\left(2+\frac{\lambda_g}{\mu_g}\right)\frac{d\phi}{dR} + \frac{\lambda_g}{\mu_g}\left(\frac{2\xi}{R}+\frac{\phi}{R}\right)\right] \sin kZ \cos 2\theta$$
$$\tau_{\theta\theta} = \left[\left(2+\frac{\lambda_g}{\mu_g}\right)\left(\frac{2\xi}{R}+\frac{\phi}{R}\right) + \frac{\lambda_g}{\mu_g}\left(\frac{d\phi}{dR}\right)\right] \sin kZ \cos 2\theta$$
$$\tau_{R\theta} = \left[\left(-\frac{2\phi}{R}+\frac{d\xi}{dR}-\frac{\xi}{R}\right)\right] \sin kZ \sin 2\theta \tag{32}$$
$$\tau_{\theta Z} = k\xi \cos kZ \sin 2\theta$$
$$\tau_{RZ} = k\phi \cos kZ \cos 2\theta.$$

Finally on inserting these stresses into the equations for radial and circumferential equilibrium, two differential equations relating ϕ and ξ are obtained:

$$\frac{d^2\phi}{dR^2}+\frac{1}{R}\frac{d\phi}{dR}-\left(1+\frac{4\mu_g}{\lambda_g+2\mu_g}\right)\frac{\phi}{R^2}-\left(\frac{\mu_g}{\lambda_g+2\mu_g}\right)k^2\phi+2\left(\frac{\lambda_g+\mu_g}{\lambda_g+2\mu_g}\right)\frac{1}{R}\frac{d\xi}{dR}$$
$$-2\left(\frac{\lambda_g+3\mu_g}{\lambda_g+2\mu_g}\right)\frac{\xi}{R^2}+\frac{2D\mu_g}{\lambda_g+2\mu_g}\frac{1}{R^3}=0 \tag{33}$$
$$\frac{d^2\xi}{dR^2}+\frac{1}{R}\frac{d\xi}{dR}-\left(1+4\frac{\lambda_g+2\mu_g}{\mu_g}\right)\frac{\xi}{R^2}-k^2\xi-2\frac{\lambda_g+\mu_g}{\mu_g}\frac{1}{R}\frac{d\phi}{dR}$$
$$-2\frac{\lambda_g+3\mu_g}{\mu_g}\frac{\phi}{R^2}+2D\frac{1}{R^3}=0.$$

The boundary conditions that must be satisfied by ϕ and ξ can be obtained from equations (32) and (29). These yield:

at $R = 1$

$$\left(2+\frac{\lambda_g}{\mu_g}\right)\frac{d\phi}{dR}+\frac{\lambda_g}{\mu_g}\left(2\frac{\xi}{R}+\frac{\phi}{R}\right) = D-1 \qquad -\frac{2\phi}{R}+\frac{d\xi}{dR}-\frac{\xi}{R} = 1$$

at $R = B$ (34)

$$\left(2+\frac{\lambda_g}{\mu_g}\right)\frac{d\phi}{dR}+\frac{\lambda_g}{\mu_g}\left(2\frac{\xi}{R}+\frac{\phi}{R}\right) = (D-4)\frac{1}{B^2}+\frac{3}{B^4} \qquad -\frac{2\phi}{R}+\frac{d\xi}{dR}-\frac{\xi}{R} = -\frac{2}{B^2}+\frac{3}{B^4}.$$

Equations (33) were solved numerically for these boundary conditions using the Gill–Kutta procedure as before and values of ϕ/R, $d\phi/dR$, ξ/R, and $d\xi/dR$ at specified radii obtained for sufficient values of n. At a given radius, the difference between the radial and circumferential stresses will be given by:

$$(\tau_{RR}-\tau_{\theta\theta}) = 2\left(\frac{d\phi}{dR}-\frac{\phi}{R}-\frac{2\xi}{R}\right)\sin kZ\cos 2\theta \tag{35}$$

and the shear stress $\tau_{R\theta}$ will be given by:

$$\tau_{R\theta} = \left(-2\frac{\phi}{R}+\frac{d\xi}{dR}-\frac{\xi}{R}\right)\sin kZ\sin 2\theta.$$

Denoting the peak value of these two quantities by h_n and i_n when k is equal to $n\pi/2T$, the difference between the radial and circumferential stresses, and the shear stress for the complete loading will be:

$$\begin{aligned}(\tau_{SS}-\tau_{\theta\theta}) &= \frac{\mu_g}{\mu_b}\left[-\frac{4}{R^2}+\frac{6}{R^4}-\frac{4}{\pi}\sum_{n=1,3,5}^{\infty}\frac{1}{n}h_n\sin\left(n\pi\frac{Z}{2T}\right)\right]\cos 2\theta\\ \tau_{R\theta} &= \frac{\mu_g}{\mu_b}\left[-\frac{2}{R^2}+\frac{3}{R^4}-\frac{4}{\pi}\sum_{n=1,3,5}^{\infty}\frac{1}{n}i_n\sin\left(n\pi\frac{Z}{2T}\right)\right]\sin 2\theta\end{aligned} \tag{36}$$

As before, the mean value of these quantities through the thickness is required, and on integration:

$$\begin{aligned}(\tau_{RR}-\tau_{\theta\theta})_{\text{mean}} &= \frac{\mu_g}{\mu_b}\left[-\frac{4}{R^2}+\frac{6}{R^4}-\frac{8}{\pi^2}\sum_{n=1,3,5}\frac{1}{n^2}h_n\right]\cos 2\theta\\ (2\tau_{R\theta})_{\text{mean}} &= \frac{\mu_g}{\mu_b}\left[-\frac{4}{R^2}+\frac{6}{R^4}-\frac{8}{\pi^2}\sum_{n=1,3,5}\frac{1}{n^2}i_n\right]\sin 2\theta\end{aligned} \tag{37}$$

On writing $B(r/a)$ and $C(r/a)$ for

$$\left(-\frac{4}{R^2}+\frac{6}{R^4}-\frac{8}{\pi^2}\sum\frac{1}{n^2}h_n\right) \quad \text{and} \quad \left(-\frac{4}{R^2}+\frac{6}{R^4}-\frac{8}{\pi^2}\sum\frac{1}{n^2}i_n\right)$$

respectively, the actual fringe order at any point in the gauge will be:

$$N = \left[B^2\left(\frac{r}{a}\right)\cos^2 2\theta + C^2\left(\frac{r}{a}\right)\sin^2 2\theta\right]^{\frac{1}{2}} \frac{\mu_g}{\mu_b}\frac{2t}{f} \tag{38}$$

In this equation and in the following equations for fringe order, the effect of rotation of the directions of principal stress through the thickness of the gauge has been neglected. The error introduced in doing this will be zero at $\theta = 0$ and $\pi/2$ and small elsewhere. A detailed discussion of this question is included in Ref. [3].

$B(r/a)$ and $C(r/a)$ are plotted against r/a for a range of values of t/a in Figs. 3 and 4 for an Araldite gauge of large outside diameter bonded onto a material of Poisson's ratio 0·3. Figures 5 and 6 show plots of $B(r/a)t/a$ and $C(r/a)t/a$ against t/a for the same gauge.

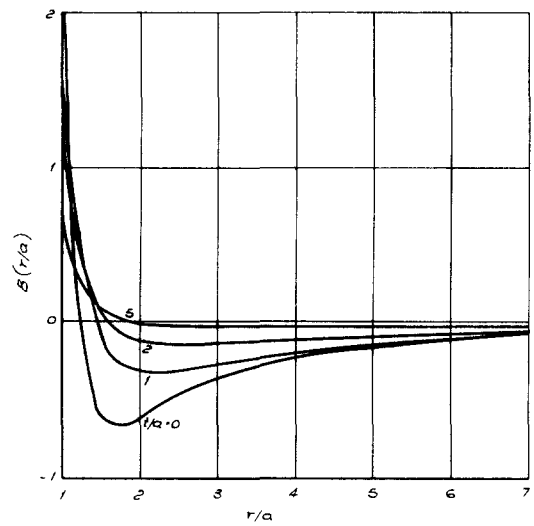

FIG. 3. Variation of $B(r/a)$ with radius.

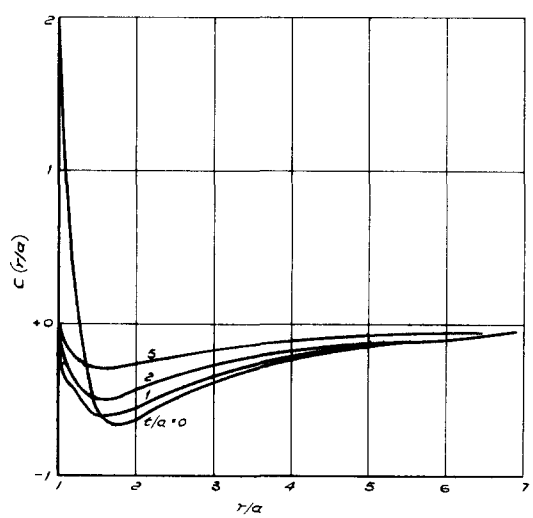

FIG. 4. Variation of $C(r/a)$ with radius.

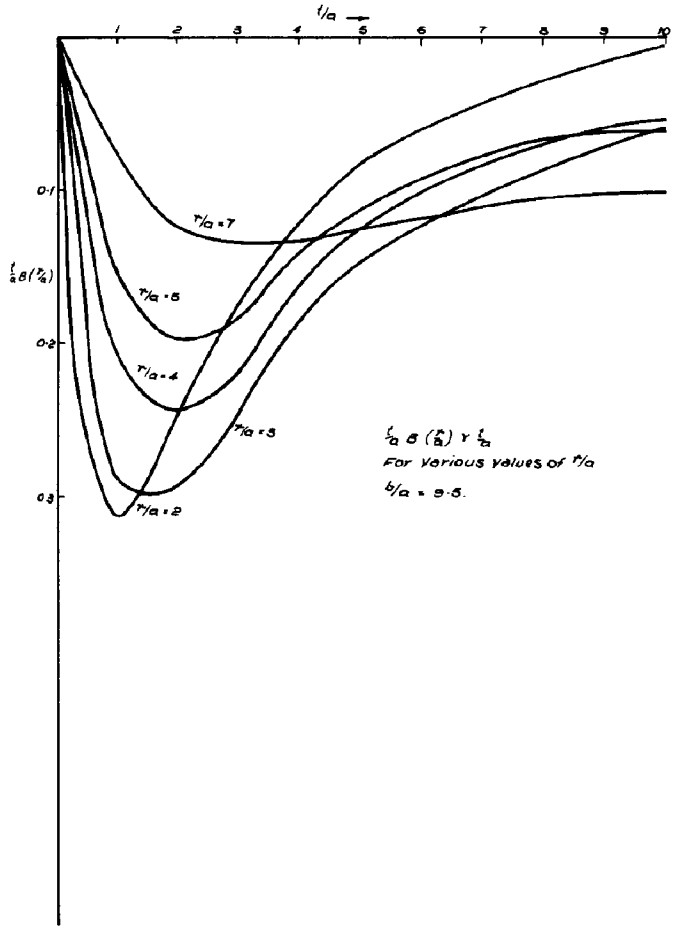

FIG. 5. Effect of gauge thickness on $t/a\ B(r/a)$.

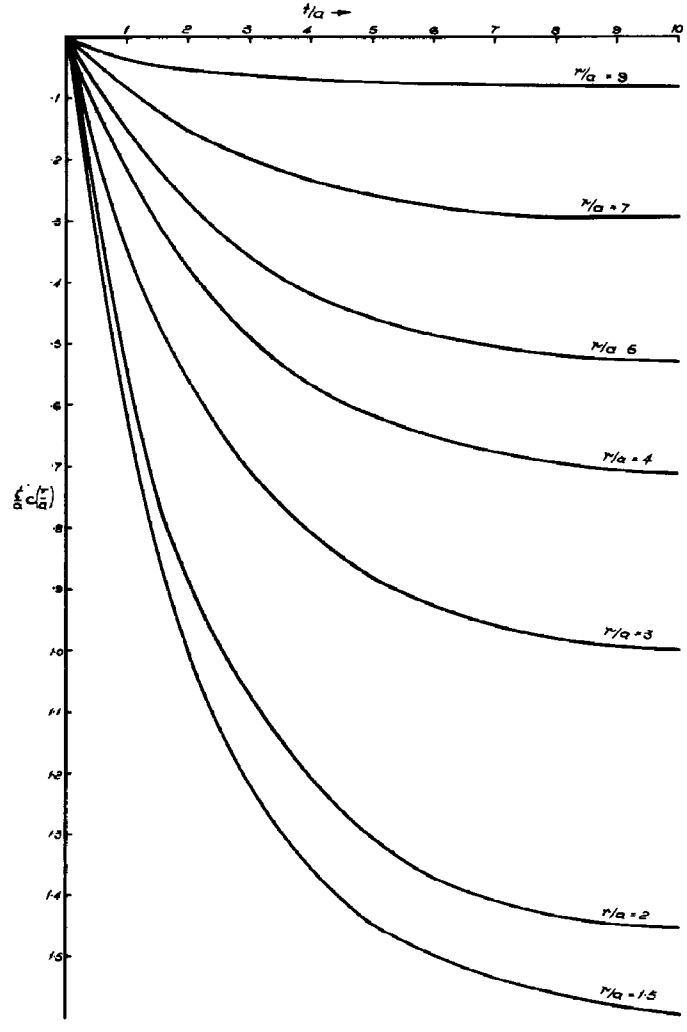

FIG. 6. Effect of gauge thickness on $t/a\ C(r/a)$.

INTERPRETATION OF FRINGE PATTERNS

Where the principal residual stresses are neither equal nor opposite the fringe order may be obtained by taking the appropriate combination of the fringe patterns for the two stress systems. For principal residual stresses given by S_1 and S_2 the fringe order at a radius r and angle θ to the stress S_1 will be:

$$N = \frac{2t}{f}\frac{\mu_g}{\mu_b}\left[\left\{\frac{S_1+S_2}{2}A\left(\frac{r}{a}\right)+\frac{S_1-S_2}{2}B\left(\frac{r}{a}\right)\cos 2\theta\right\}^2+\frac{S_1-S_2}{2}C\left(\frac{r}{a}\right)\sin 2\theta^2\right]^{\frac{1}{2}} \tag{39}$$

It follows that the directions of the principal residual stresses coincide with the axes of symmetry of the fringe pattern. Also the fringe orders at specific radii on the axes of symmetry, and on the line at 45° to them, are related to the principal residual stresses by the equations:

$$N_1 = \frac{2t}{f}\frac{\mu_g}{\mu_b}\left[\frac{S_1+S_2}{2}A\left(\frac{r}{a}\right)+\frac{S_1-S_2}{2}B\left(\frac{r}{a}\right)\right] \tag{40a}$$

$$N_2 = \frac{2t}{f}\frac{\mu_g}{\mu_b}\left[\frac{S_1+S_2}{2}A\left(\frac{r}{a}\right)-\frac{S_1-S_2}{2}B\left(\frac{r}{a}\right)\right] \tag{40b}$$

$$N_3 = \frac{2t}{f}\frac{\mu_g}{\mu_b}\left[\left(\frac{S_1+S_2}{2}A\left(\frac{r}{a}\right)\right)^2+\left(\frac{S_1-S_2}{2}C\left(\frac{r}{a}\right)\right)^2\right]^{\frac{1}{2}} \tag{40c}$$

where

N_1 is the fringe order measured where $\theta = 0°$

N_2 is the fringe order measured where $\theta = 90°$

N_3 is the fringe order measured where $\theta = 45°$

S_1 is the residual stress acting in direction $\theta = 0°$

S_2 is the residual stress acting in direction $\theta = 90°$

Using these equations the principal residual stresses can be found in terms of N_1 and N_2 by re-arranging the first two of these equations.

i.e.

$$S_1 = \frac{f}{2t}\frac{\mu_b}{\mu_g}\left[\frac{1}{2}N_1\frac{A(r/a)+B(r/a)}{A(r/a)B(r/a)}+\frac{1}{2}N_2\frac{B(r/a)-A(r/a)}{A(r/a)B(r/a)}\right]$$

$$S_2 = \frac{f}{2t}\frac{\mu_b}{\mu_g}\left[\frac{1}{2}N_2\frac{A(r/a)+B(r/a)}{A(r/a)B(r/a)}+\frac{1}{2}N_1\frac{B(r/a)-A(r/a)}{A(r/a)B(r/a)}\right].$$

Alternatively the sum of the residual stresses can be obtained from equations (40a and b) and the difference obtained using equation (40c). This enables a check to be made on the accuracy of the measurement. The equations for the principal residual stresses in this case

are:

$$S_1 = \frac{f}{2t}\frac{\mu_b}{\mu_g}\left[\frac{N_1+N_2}{2}\frac{1}{A(r/a)}+\left\{N_3^2-\left(\frac{N_1+N_2}{2}\right)^2\right\}^{\frac{1}{2}}\frac{1}{C(r/a)}\right]$$

$$S_2 = \frac{f}{2t}\frac{\mu_b}{\mu_g}\left[\frac{N_1+N_2}{2}\frac{1}{A(r/a)}-\left\{N_3^2-\left(\frac{N_1+N_2}{2}\right)^2\right\}^{\frac{1}{2}}\frac{1}{C(r/a)}\right]$$

Values of $(A+B/AB$ and $(B-A)/AB$ have been plotted in Fig. 7 against r/a for $b/a = 5$ and $t/a = 1{\cdot}5$ for Araldite gauges bonded onto a material with a Poisson's ratio of 0·28.

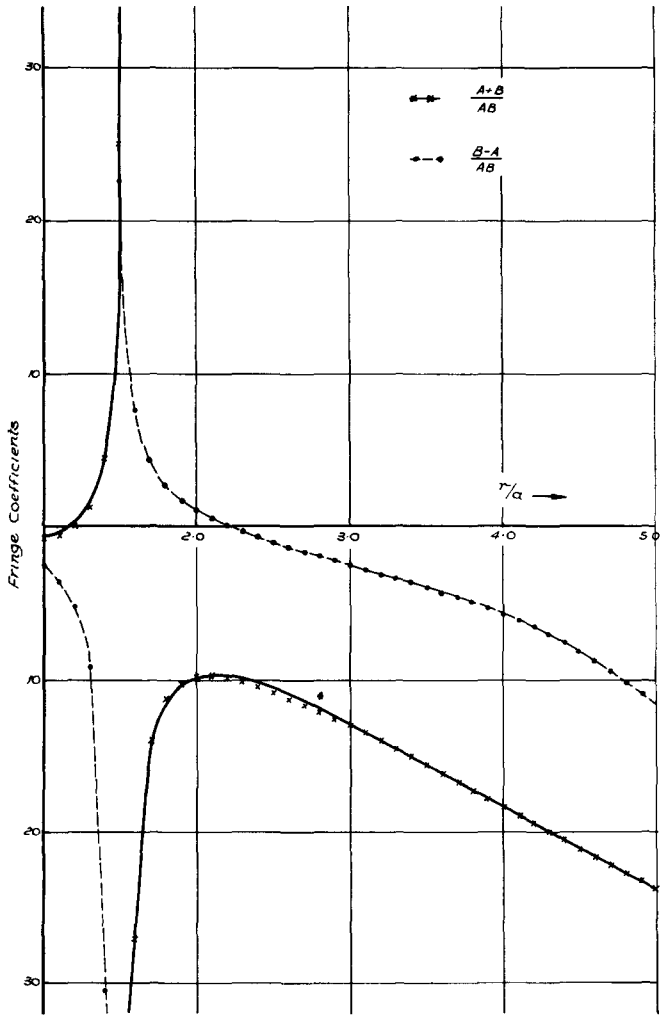

FIG. 7. Fringe coefficients $(A+B)/AB$ and $(B-A)/AB$.

DISCUSSION OF RESULTS

Figures 1, 3 and 4 show plots of $A(r/a)$, $B(r/a)$ and $C(r/a)$ against r/a for a range of values of t/a. The curves for $t/a = 0$ represent the values that would be obtained neglecting shear lag. It can be seen that even for relatively thin gauges of t/a of 1 the error produced by neglecting the shear lag effect is considerable, and would in practice lead to an underestimation of the residual stresses of about 50%.

From Fig. 2 in which t/a $A(r/a)$ is plotted against t/a, it is apparent that as the gauge thickness is increased from zero, the fringe order produced by a unit equiaxial residual stress increases, rapidly at first, but at a decreasing rate, until eventually further increases in gauge thickness produce no corresponding increase in fringe order.

A similar result is found for the case of equal but opposite unit residual stresses, Figs. 5 and 6, except that the effect is somewhat complicated by the more complex relationship of fringe order to radius. In practice there is little point in making the gauge thickness greater than the hole diameter and for an investigation of the effect of the ratio b/a a value of t/a of 1·5 was adopted.

In Figs. 8, 9 and 10 the coefficients $A(r/a)$, $B(r/a)$ and $C(r/a)$ are plotted against r/a for a range of values of the ratio of the outside radius to the inside radius of the gauge for $t/a = 1{\cdot}5$.

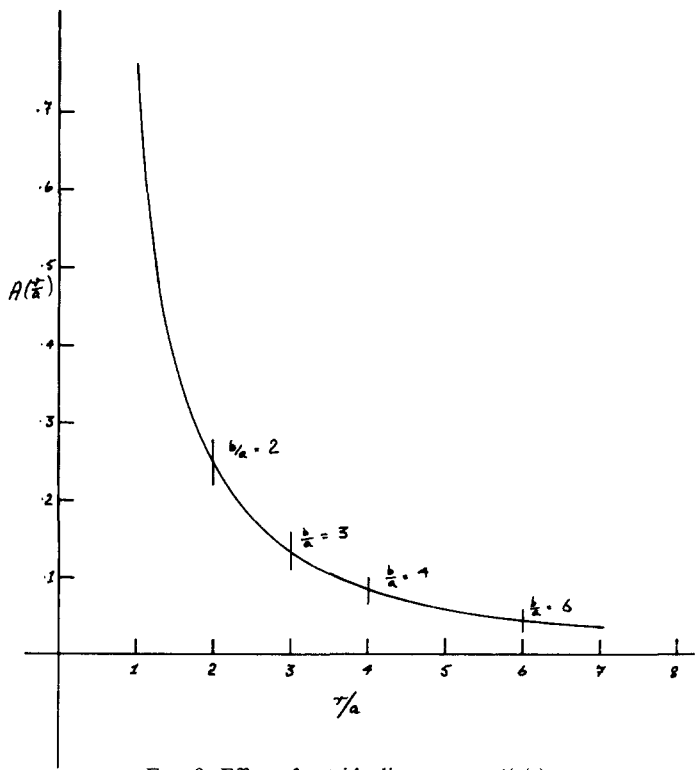

FIG. 8. Effect of outside diameter on $A(r/a)$.

The outside diameter of the gauge has no effect on $A(r/a)$ and little effect on $C(r/a)$ except at points close to the gauge outside diameter. For $B(r/a)$ on the other hand the ratio

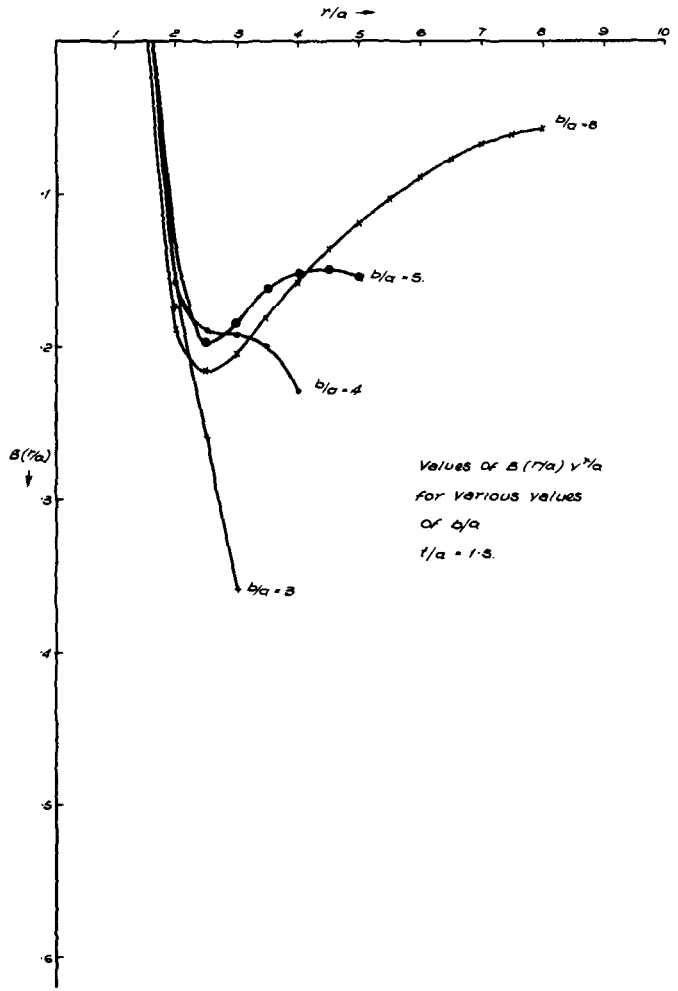

FIG. 9. Effect of outside diameter on $B(r/a)$.

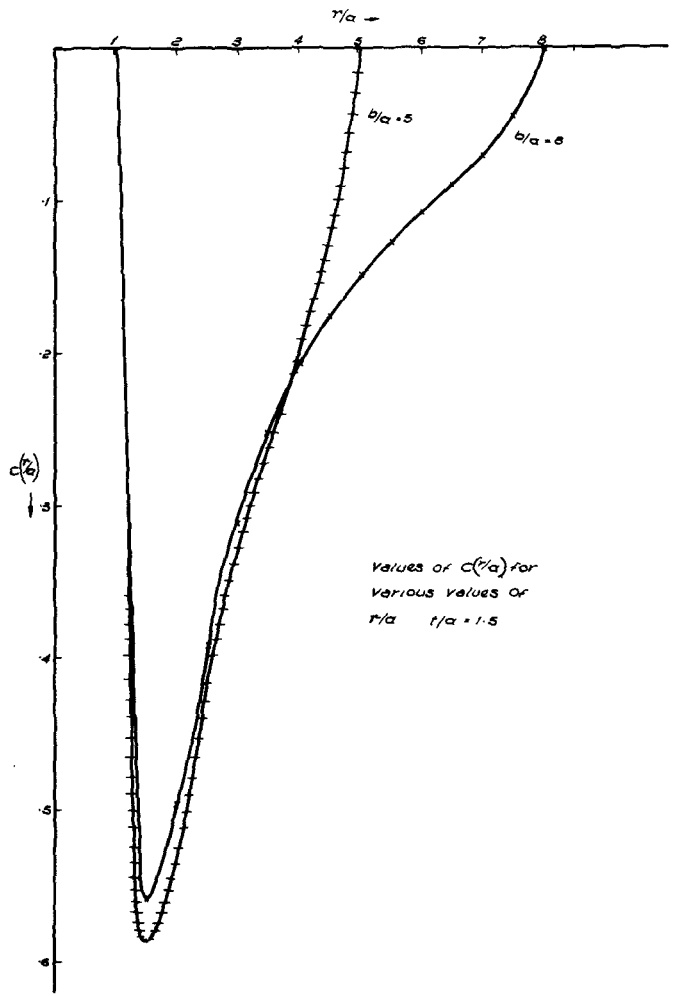

FIG. 10. Effect of outside diameter on $C(r/a)$.

b/a has a considerable effect, and the influence of the position of the outer surface on the value of $B(r/a)$ at $r/a = 2$, (the point adopted for measuring fringe orders in practical applications) does not become negligible until b/a is greater than 8. In view of the uncertainty of the exact position of the outer boundary due to a fillet of bonding material that is of necessity present, the outside diameter of the gauge must be as large as possible. In practice a value of b/a of 5 was adopted as a compromise between the requirements of a small physical gauge size for practical application and a large gauge size for accuracy.

PRACTICAL ASPECTS—GAUGE MANUFACTURE AND APPLICATION

The gauge material selected was Araldite hot cure resin C.T. 200, mainly because the authors had extensive experience in the use of this material for photoelastic work.

The method of manufacture was simple. Cylindrical casts of C.T. 200 1·5 in. dia. and about 12 in. long were prepared. The diameter was then machined to 1·25 in. and a 0·242 in. dia. hole drilled accurately along the axis of the cylinder. Gauges 0·187 in. thick were then parted off using a diamond impregnated slitting wheel mounted on a modified surface grinding machine. The gauge faces were polished using 600 grit paper and finally a six micron wheel. Lastly the central holes in the gauges were brought to 0·250 in. dia. using a hand reamer.

The gauges were cemented to the surface using Photo-elastic Incorporated P.C.10 adhesive which is a relatively fast curing epoxide containing a reflective filler.

In order to locate the centre of the drilled hole a drill bush 0·250 in. o.d. and 0·125 in. i.d. was placed through the hole in the gauge. A 1/8 in. dia. pilot hole was then drilled into the material under investigation. Material was then removed in stages with a range of drills increasing in diameter. The final drilled hole (0·242 in. dia.) was then reamed to 0·250 in., care being taken not to touch the gauge excessively.

EXPERIMENTAL VERIFICATION

Experimental work has been conducted to verify the theoretical analysis. A high strength aluminium alloy bar of $1{\cdot}25 \times 0{\cdot}25$ in. cross-section was loaded in a tensile testing machine to a load of 2 ton (6·4 ton/in^2) and photoelastic gauges cemented to its surface. The bar was then unloaded and the 0·25 in. dia. central holes drilled through the bar and reamed as described in the previous section. After reloading, the fringe orders were measured on radii parallel, normal, and at 45° to the direction of loading at points one hole radius away from the hole boundary. The mean of the two, or four fringe orders was taken in each case.

The experimental results obtained are presented in Table 1, the mean of the values of the fringe orders from a number of gauges being shown. In the same table the values of the

TABLE 1

	Experiment	Shear lag theory	Uncorrected theory
Parallel	0·8	0·82	2·19
Normal	0·3	0·14	0·25
45°	1·3	1·13	1·56

fringe orders predicted using the theory presented here, and the values predicted without allowing for the effect of "shear lag" are presented for comparison. The maximum difference at any position between the experimental results and those predicted allowing for the effect of "shear lag" was 0·17 fringe orders; the maximum difference between the experimental results and those predicted without allowing for the effect of shear lag was 1·4 fringe orders.

Thus taking as 100% the maximum experimental fringe order (1·3), the percentage error has been reduced from 107% to 13% and is now within the normal experimental errors associated with the method.

CONCLUSIONS

The "shear lag" effect in photoelastic gauges can lead to considerable errors in the determination of residual stress unless allowance is made for it in relating fringe orders to stress. Using the approximate theory presented in this paper these errors are reduced below the normal experimental errors associated with the photoelastic method of measuring residual stresses.

Acknowledgement—The authors wish to thank the directors of Joseph Lucas Ltd. for permission to publish the experimental results presented in this paper.

REFERENCES

[1] M. NISIDA, A method of stress measurement. *Br. Pat. Spec.* **938**, 289 (1963).
[2] M. NISIDA and H. TAKABAYASHI, Thickness effects in "hole method" and applications of the method to residual stress measurement. *Proc. 13th Japan Natn. Congr. appl. Mech.* 1963, p. 108.
[3] H. G. GIBBS, C. J. HOOKE and J. J. STAGG, An application of photoelastic gauges to the measurement of residual stress. *VDI-Ber.* No. 102 (1966).
[4] L. N. G. FILON, On the elastic equilibrium of circular cylinders under certain practical systems of loads. *Phil. Trans. R. Soc.* **A198**, 147 (1902).
[5] B. G. GALERKIN, Elastic equilibrium of a hollow circular cylinder and parts of a cylinder. *Collected Works*, Vol. 1, p. 342 (1952).
[6] V. K. PROKOPOV, Equilibrium of an elastic thick walled axisymmetric cylinder. *Prikl. Mat. Mekh.* **12**, 135 (1949).
[7] M. W. BARTON, The circular cylinder with a band of uniform pressure on a finite length of the surface. *J. appl. Mech.* **8**, 97 (1941).
[8] A. I. LUR'E, *Three Dimensional Problems in the Theory of Elasticity*. Interscience (1964).
[9] I. S. SOKOLNIKOFF, *Mathematical Theory of Elasticity*. McGraw-Hill (1956).

(*Received* 13 *March* 1967; *revised* 19 *May* 1967)

Абстракт—Дается приближенный метод, который допускает эффект чеппанащей ом сдвига в фотоупругих датчиках. Приводятся численные расуеты для широкого масштаба геометрий датчиков.